SPECIAL
U.S. CLIVAR Hurricanes
COLLECTION

Resolution Dependence of Future Tropical Cyclone Projections of CAM5.1 in the U.S. CLIVAR Hurricane Working Group Idealized Configurations

MICHAEL WEHNER AND PRABHAT

Computational Research Division, Lawrence Berkeley National Laboratory, Berkeley, California

KEVIN A. REED

National Center for Atmospheric Research, Boulder, Colorado*

DÁITHÍ STONE AND WILLIAM D. COLLINS

Computational Research Division, Lawrence Berkeley National Laboratory, Berkeley, California

JULIO BACMEISTER

National Center for Atmospheric Research, Boulder, Colorado*

(Manuscript received 29 April 2014, in final form 18 January 2015)

ABSTRACT

The four idealized configurations of the U.S. CLIVAR Hurricane Working Group are integrated using the global Community Atmospheric Model version 5.1 at two different horizontal resolutions, approximately 100 and 25 km. The publicly released 0.9° × 1.3° configuration is a poor predictor of the sign of the 0.23° × 0.31° model configuration's change in the total number of tropical storms in a warmer climate. However, it does predict the sign of the higher-resolution configuration's change in the number of intense tropical cyclones in a warmer climate. In the 0.23° × 0.31° model configuration, both increased CO_2 concentrations and elevated sea surface temperature (SST) independently lower the number of weak tropical storms and shorten their average duration. Conversely, increased SST causes more intense tropical cyclones and lengthens their average duration, resulting in a greater number of intense tropical cyclone days globally. Increased SST also increased maximum tropical storm instantaneous precipitation rates across all storm intensities. It was found that while a measure of maximum potential intensity based on climatological mean quantities adequately predicts the 0.23° × 0.31° model's forced response in its most intense simulated tropical cyclones, a related measure of cyclogenesis potential fails to predict the model's actual cyclogenesis response to warmer SSTs. These analyses lead to two broader conclusions: 1) Projections of future tropical storm activity obtained by a direct tracking of tropical storms simulated by coarse-resolution climate models must be interpreted with caution. 2) Projections of future tropical cyclogenesis obtained from metrics of model behavior that are based solely on changes in long-term climatological fields and tuned to historical records must also be interpreted with caution.

1. Introduction

The Hurricane Working Group (HWG) of the U.S. Climate Variability and Predictability Research Program (CLIVAR) proposed a set of four idealized configurations for atmospheric general circulation models (AGCMs) to explore the effects of increased sea surface temperature (SST) and increased atmospheric carbon dioxide concentrations both separately and jointly on future tropical storm behavior in

Denotes Open Access content.

* The National Center for Atmospheric Research is sponsored by the National Science Foundation.

Corresponding author address: Michael Wehner, Computational Research Division, Lawrence Berkeley National Laboratory, 1 Cyclotron Rd., Berkeley, CA 94720.
E-mail: mfwehner@lbl.gov

DOI: 10.1175/JCLI-D-14-00311.1

a warmer climate (http://www.usclivar.org/working-groups/hurricane; Held and Zhao 2011). The base configuration, called CLIMO in this paper, calls for a multiyear integration of AGCMs with the surface boundary conditions (SST and sea ice extent) set to early 1990s average values and atmospheric carbon dioxide (CO_2) concentrations set to 330 ppm. The second configuration, called SSTplus2 here, simply adds 2°C uniformly to the SSTs. The third configuration, called 2xCO2, uses the 1990 surface climatology but doubles the CO_2 concentration to 660 ppm. The fourth configuration, called SSTplus2_2xCO2, combines the uniform addition of 2°C to the 1990 climatological SST and 660 ppm value of atmospheric CO_2. Sulfate and other trace aerosol concentrations are fixed to 2000 climatological values from a related coupled model simulation and are the same for all experiments. Analyses in this paper are confined to global measures of tropical storm behavior. While the potential for different responses to forcing changes in different basins is significant, such differences are likely to depend on the details of the spatial pattern of forcing changes. As the U.S. CLIVAR HWG forcing changes are spatially uniform, detailed basin analyses are deferred until more realistic simulations of a future climate are performed.

The motivation for this particular set of simulation experiments is to understand the effects of increased available ocean heat energy on tropical cyclogenesis and development, and the potential competing effect of the vertical stabilization of the atmosphere by increased CO_2 levels following the pioneering work of Yoshimura and Sugi (2005). The Fifth Assessment Report of the Intergovernmental Panel on Climate Change stated "...it is *likely* that the global frequency of occurrence of tropical cyclones will either decrease or remain essentially unchanged..." (Christensen et al. 2013, p. 14-4). However at present, there is no compelling quantitative theory explaining the relationship between the state of the climate system and tropical cyclone formation (Walsh et al. 2015). As a result, climate models that can actually produce storms resembling tropical cyclones are the only tools that can currently provide information about the behavior of such storms in future climates. Previous work suggests that confidently assessing projected future changes in tropical cyclones is complex as conclusions vary depending on both the details of the climate models and the experimental configuration (Knutson et al. 2010). The U.S. CLIVAR HWG experimental suite provides a common experimental framework to isolate model-dependent responses. Preliminary multimodel results have been reported in Zhao et al. (2013), Daloz et al. (2015), Shaevitz et al. (2014), and Walsh et al. (2015).

Although overly simplified, these four numerical experiments begin to provide a basis to develop a climate theory of tropical cyclone formation (Walsh et al. 2015). Sugi et al. (2012) argued that an increase in CO_2 decreases radiative cooling, precipitation, and upward mass flux, leading to a decrease in tropical storm frequency, and that a uniform increase in SST increases atmospheric stability together with an additional decrease in the upward mass flux, also leading to a decrease in tropical storm frequency. This paper explores in detail the tropical storm statistics of a single model, the Community Atmospheric Model version 5.1 (CAM5.1), at two different horizontal resolutions in the four U.S. CLIVAR HWG idealized configurations and provides insight into the relative roles of increased ocean temperature and greenhouse gases on future tropical storm behavior as well as some guidance to the interpretation of multimodel datasets, including the current generation of the Coupled Model Intercomparison Project, CMIP5.

2. The Community Atmospheric Model and simulated tropical cyclone performance

The Community Atmospheric Model developed by the U.S. Department of Energy and the National Science Foundation is one of several global atmospheric models currently being run at resolutions in the 60–25-km range to simulate past and future tropical storm statistics (Yoshimura and Sugi 2005; Oouchi et al. 2006; Zhao et al. 2009; Sugi et al. 2009; Yamada et al. 2010, Strachan et al. 2013; Wehner et al. 2014). The version of the model described in this study uses the finite volume dynamical core on a latitude–longitude mesh and is the publicly released version CAM5.1 (Neale et al. 2010). The standard resolution is 0.9° (latitude) by 1.3° (longitude) or approximately 100 km at the equator. This paper describes results from the four HWG configurations at both this resolution and at the higher resolution of 0.23° by 0.31° or approximately 25 km at the equator. The parameters in the finite-volume dynamics scheme and in all of the subgrid-scale physical parameterizations are the same at both model resolutions with the exception of the dynamics and physics time steps (Wehner et al. 2014). The values of the unaltered parameters were taken from the tuned public release of the model at the standard resolution and no additional tuning was performed for this study at either resolution. The two resolutions will be referred to as $0.9° \times 1.3°$ and $0.23° \times 0.31°$ throughout this paper. The vertical resolution was unchanged at 30 levels with the model top at about 2 hPa.

The model's mean and extreme value climatologies at both resolutions are described in Bacmeister et al.

(2014) and Wehner et al. (2014) using the Atmospheric Model Intercomparison Project (AMIP) protocols. AMIP experiments differ from the U.S. CLIVAR HWG experiments in that the external forcings (surface boundary conditions, solar insolation, and atmospheric trace compound concentrations) are prescribed as realistically time-varying functions rather than the fixed seasonal climatology cases described in this study. These two studies revealed that the CAM5.1 tropical storm climatology in the 0.23° × 0.31° model configuration compares well with observations. Using the 0.23° × 0.31° mesh, CAM5.1 produced 83 ± 8 tropical storms per year (sustained winds greater than 17.5 m s^{-1}), 52 ± 4 tropical cyclones (in this paper "tropical cyclones" are defined to have sustained winds greater than 33 m s^{-1} defined as category 1 or greater on the Saffir–Simpson scale), and 9 ± 1.6 intense tropical cyclones per year (sustained winds greater than 58 m s^{-1} defined as categories 4 and 5 on the Saffir–Simpson scale) over the entire globe in a 1979–2005 simulation following the AMIP protocols. The uncertainties specified in annual storm numbers is determined by the 5%–95% confidence range based on interannual variability. The observed numbers per year from the (IBTrACS) observed track database (Knapp et al. 2010) during this period were 85 tropical storms, 48 tropical cyclones, and 28 intense tropical cyclones over all ocean basins. The simulated storm counts were produced using the tracking algorithm from the Geophysical Fluid Dynamics Laboratory (GFDL) with the threshold values for vorticity, warm core temperature anomaly, and planetary boundary layer depth as in Knutson et al. (2007) modified to run on highly parallel systems (Prabhat et al. 2012). An observational estimate of tropical storm tracks is shown in the appendix (see Fig. A1) for comparison.

The CLIMO experiment results in very nearly the same tropical storm climatology as does an AMIP experiment. The model exhibits acceptable seasonal behaviors in the North Atlantic, eastern and western North Pacific, and northern Indian Ocean basins. In the CLIMO experiment, the 0.23° × 0.31° model produces approximately the correct number of storms per year in each of the well-observed ocean basins, with the most significant bias being that too many storms form in the central Pacific, resulting in counts being too low in the West North Pacific and too high in the northeast Pacific, although the total number of North Pacific storms is reasonable. As in the observations, most of the simulated tropical storms, especially those of category 4 wind speeds or greater, occur in the Pacific basin. The present study examines changes in global tropical storm intensities and frequencies. The biases in Pacific cyclogenesis location, while important when considering the impacts of landfall and other localized details of tropical storm statistics, are not expected to have a significant effect on the forced response in global tropical storm statistics due to the uniform forcing changes imposed in this study. The model's simulated tropical storm behavior at both resolutions from the AMIP simulations is described more completely in Wehner et al. (2014).

In contrast, the 0.9° × 1.3° model produces far too few tropical storms when the detection parameters are unchanged from Knutson et al. (2007). At this resolution, the model produced only 8.9 ± 1.5 tropical storms per year during a simulation of the 1979–2005 period. The model behavior in replicating observations during this period is discussed at length in Wehner et al. (2014). The deficiency in the number of tropical storms at a lower resolution is also consistent with idealized studies using similar versions of CAM (Reed and Jablonowski 2011b; Reed et al. 2012). In those studies it is demonstrated that the model has the ability of simulating tropical cyclones at horizontal resolutions of 0.5° or less, and struggles to simulate storms at coarser resolutions, using an idealized vortex initialization technique (Reed and Jablonowski 2011a). We note that the effect of higher resolution on the simulation of tropical storm statistics can be very specific to the model and tracking algorithm. For instance, while simulated peak wind speeds in the 0.23° × 0.31° version of CAM5.1 are very similar to those in the MRI-AGCM20_3.2version of the Meteorological Research Institute's ~20-km model (Murakami et al. 2012), they are considerably higher than in the Hadley Centre Global Environmental Model version 1 (HadGEM1), albeit at the coarser resolution of ~60 km (Strachan et al. 2013). However, the number of tracked storms in the both the ~90- and ~135-km version of HadGEM1 were found to be higher and closer to observations using the Hodges (1996) tracking algorithm than in the 0.9° × 1.3° version of CAM5.1 using the GFDL tracking algorithm.

3. Forced changes in the annual number of tropical storms

The 0.9° × 1.3° version of CAM5.1 was integrated for at least 24 yr in each of the four U.S. CLIVAR HWG configurations. In this study, the first year of each simulation is discarded to allow the model ample time to spin up to the experimental forcing configuration. Also, the tropical storm tracking parameters are as defined in Knutson et al. (2007) and repeated in Wehner et al. (2014). Tropical storm statistics simulated by the 0.9° × 1.3° version CAM5.1 in the CLIMO experiment are very similar to those obtained in the AMIP experiment at this resolution described in Wehner et al. (2014) and produced on average 8.6 ± 1.3 events that reached tropical

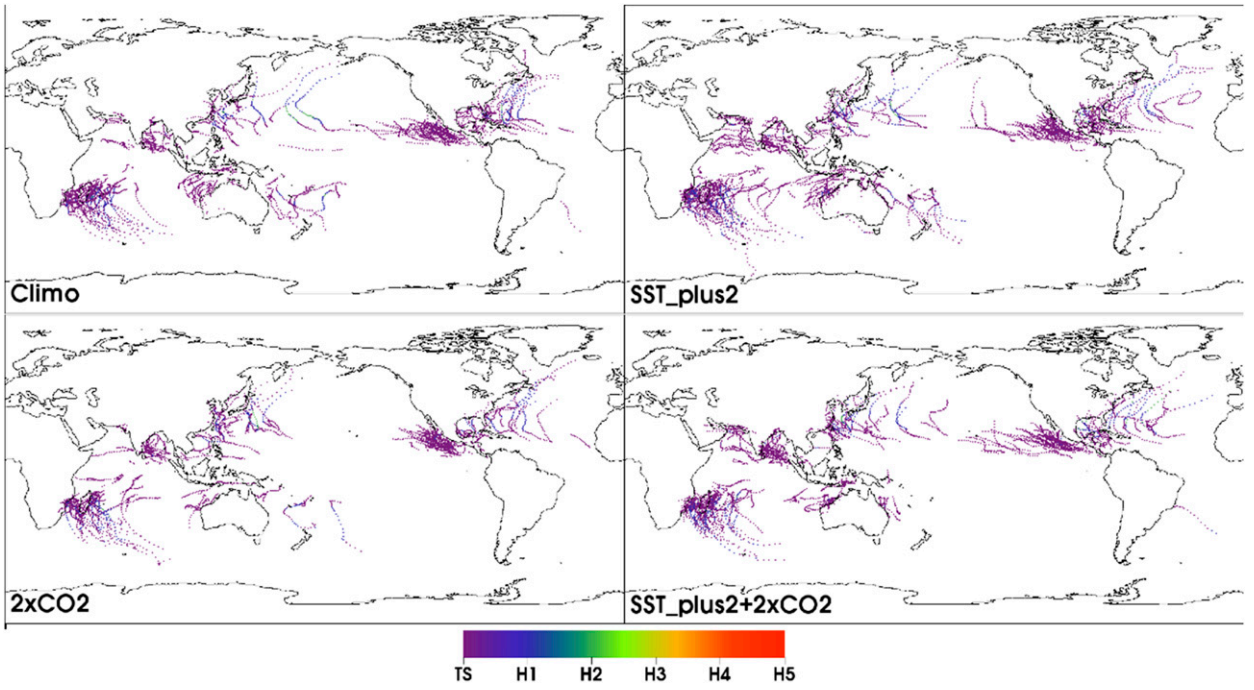

FIG. 1. Tropical storm tracks over the final 23 simulated years for the U.S. CLIVAR HWG experiments produced by the 0.9° × 1.3°CAM5.1 configuration. Colors indicate storm intensity.

storms wind speeds per year of which 2.25 ± 1.5 per year reached tropical cyclone winds speeds. Category 2 wind speeds ($43\,m\,s^{-1}$) are reached in fewer than half of the simulated years. The strongest storm tracks over the final 23 simulated years are shown in the upper left panel of Fig. 1 for this resolution under the CLIMO forcing.

Increasing only the SST by 2°C in the SSTplus2 experiment causes the 0.9° × 1.3° model to produce more storms, 11.4 ± 1.7 tropical storms per year. Storm tracks over the final 23 years of the SSTplus2 simulation are shown in upper right panel of Fig. 1. This result is different from the CLIMO experiment at a 99% significance level using a two-sided Student's *t* test. (A two-sided test is used as it plausible that the difference could be either positive or negative.) Increasing only atmospheric CO_2 to 660 ppm in the 2xCO2 experiment causes the 0.9° × 1.3° model to produce fewer storms, 7.5 ± 0.9 tropical storms per year. Storm tracks over the final 23 years of the 2xCO2 simulation are shown in lower left panel of Fig. 1. This result is different from the CLIMO experiment at a 78% significance level using a two-sided Student's *t* test. Increasing both forcings in the SSTplus2_2xCO2 experiment causes the 0.9° × 1.3° model to produce more storms, 10.1 ± 1.4 tropical storms per year. Storm tracks over the final 23 years of the SSTplus2_2xCO2 simulation are shown in lower right panel of Fig. 1. This result is different from the CLIMO experiment at an 89% significance level using a two-sided Student's *t* test. These differences are summarized in Fig. 2 where the error bars represent the 5%–95% confidence interval estimates of the average number of tropical storms per year.

The changes in annual tropical storm numbers are very different in the 0.23° × 0.31° version of CAM5.1 than the 0.9° × 1.3° version. Because of the high computational costs and resources limitations, the 0.23° × 0.31° model was integrated for shorter periods ranging from 14 to 17 years. However, because of a larger, more realistic number of simulated storms per year and the smaller interannual variations relative to this number, the statistical significance between the different HWG configurations is actually larger for the 0.23° × 0.31° model. In the last 13 years of the 0.23° × 0.31° CLIMO experiment, the model annually produces 86 ± 4 storms of tropical storm strength or greater (categories 0–5), 44 ± 2.6 of tropical cyclone strength (categories 1–3) and 10 ± 1.7 intense tropical cyclones (categories 4 and 5) with a track distribution, shown in upper left panel of Fig. 3, similar to that reported in Wehner et al. (2014).

Increasing only the SST by 2°C in the SSTplus2 experiment causes the 0.23° × 0.31° model to annually produce fewer total storms of tropical storm strength or greater (82.5 ± 4) compared to the CLIMO experiment. This is in contrast to the increase in total storm numbers exhibited by the 0.9° × 1.3° model under the same forcing change. The number of storms of tropical

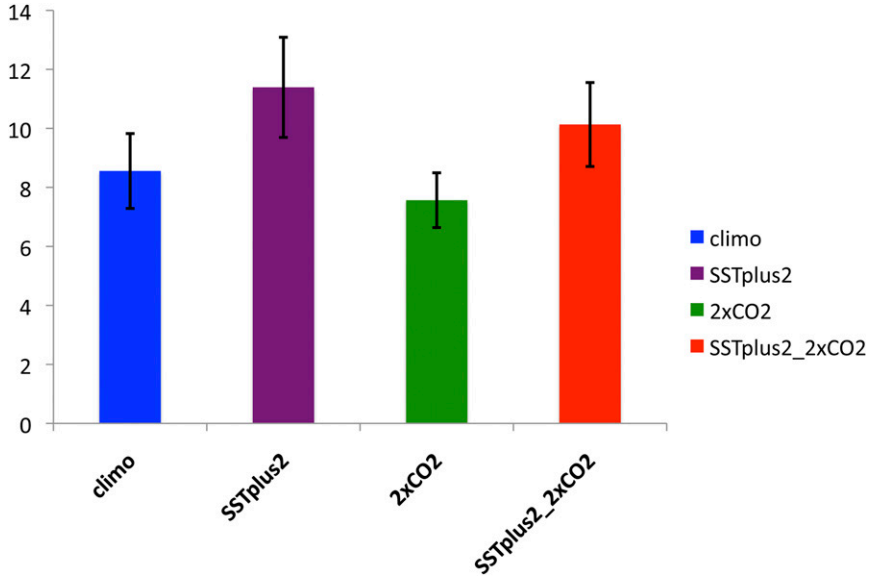

FIG. 2. Global average number of tropical storms per year simulated by the 0.9° × 1.3° version of CAM5.1 for the four U.S. CLIVAR HWG idealized AGCM configurations. Error bars represent 5%–95% confidence intervals based on interannual variability.

cyclone strength is 42 ± 3 and is not statistically significantly different but the number of storms of intense tropical cyclone strength is increased to 14 ± 1.2. The decrease in the total number of storms in the SSTplus2 experiment from the CLIMO experiment is significant at the 81% level using a two-sided Student's *t* test for the 0.23° × 0.31° model. The significance of the increase in the annual number of intense tropical cyclones exceeds a 99% level for SSTplus2 experiment compared to the CLIMO experiment using a similar test for the

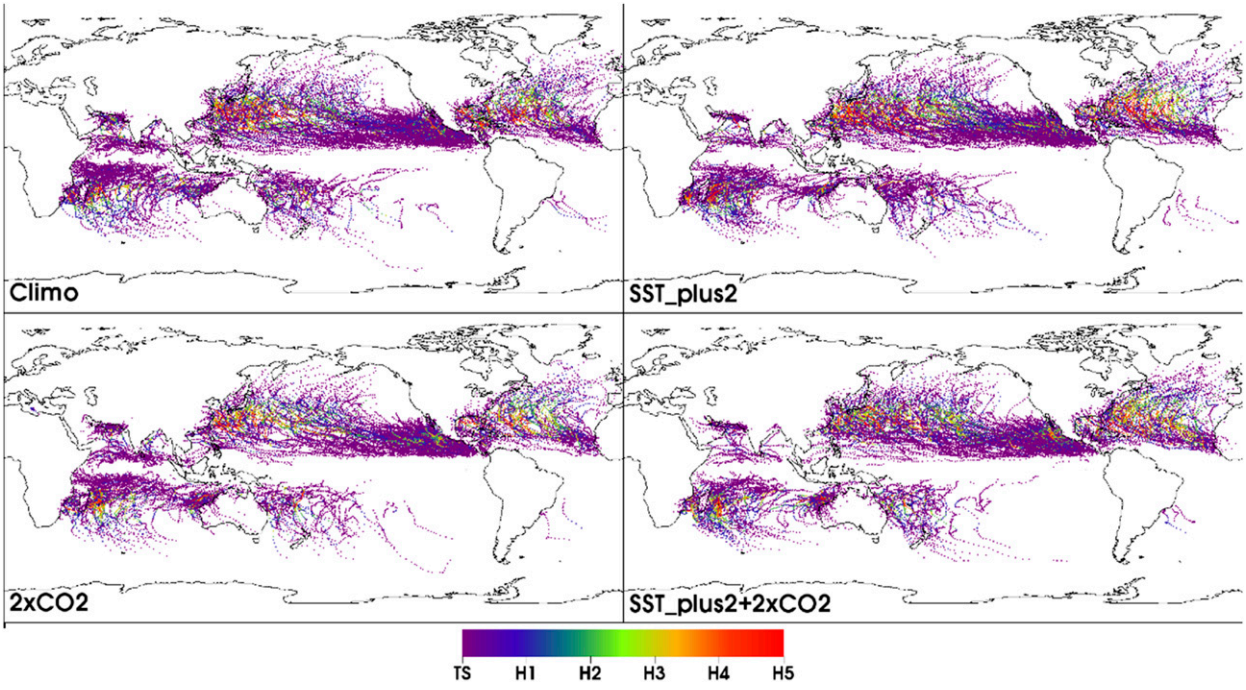

FIG. 3. Tropical storm tracks over the final 13 simulated years for the U.S. CLIVAR HWG experiments produced by the 0.23° × 0.31° CAM5.1 configuration. Colors indicate storm intensity.

0.23° × 0.31° model. The upper right panel of Fig. 3 shows the tracks for the last 13 years of the SSTplus2 experiment for the 0.23° × 0.31° model.

Compared to the CLIMO experiment, increasing only the atmospheric CO_2 concentration to 660 ppm in the 2xCO2 experiment substantially reduces the annual number of tropical storms to 72 ± 4, of tropical cyclone strength to 37 ± 3, and of intense tropical cyclone strength to 7 ± 1.6 for the 0.23° × 0.31° model. This reduction in total annual number compared to the CLIMO experiment is similar to the 0.9° × 1.3° model experiments and is significant at over a 99% level at the higher-resolution experiments. Likewise the reduction in annual numbers of tropical cyclones is also significant at over a 99% level. The decrease in intense tropical cyclones is significant at the 94% level using the same two-sided Student's *t* test. The lower left panel of Fig. 3 shows the tracks for the last 13 yr of the 2xCO2 experiment for the 0.23° × 0.31° model.

Finally, imposing both forcing changes in the SSTplus2_2xCO2 experiment reduces the total annual number of tropical storms to 70 ± 3 and the number of tropical cyclone strength storms to 39 ± 2 compared to the CLIMO experiment for the 0.23° × 0.31° model. However, the annual number of intense tropical cyclones is increased compared to the CLIMO experiment to 12 ± 1.7 when both forcings are applied. Similar to the SSTplus2 experiments, this reduction of total annual number for the 0.23° × 0.31° model is also in contrast to the equivalent experiment at 0.9° × 1.3° and is significant at over a 99% level. The reduction of the annual number of tropical cyclones is also significant at over a 99% level. Because the effects on intense tropical cyclones of increasing SST and CO_2 concentrations are of opposite signs, the net increase in the annual number of intense tropical cyclones is significant at a only an 84% level using the same two-sided Student's *t* test as above. Tracks for the SSTplus2_2xCO2 experiment are shown in the lower right panel of Fig. 3 for the 0.23° × 0.31° model. These differences in storm counts between the four 0.23° × 0.31° model experiments are summarized in Fig. 4.

The signs of the changes discussed above are summarized in Table 1 for the two model resolutions. Comparison of the top row with the middle row reveals that the 0.9° × 1.3° model's response to forcing changes

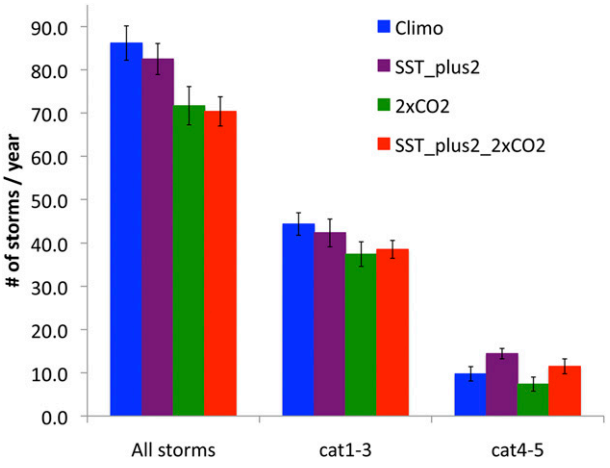

FIG. 4. Global average number of tropical storms, tropical cyclones and intense tropical cyclones per year simulated by the 0.23° × 0.31° version of CAM5.1 for the four U.S. CLIVAR HWG idealized AGCM configurations. Error bars represent 5%–95% confidence intervals based on interannual variability.

is a poor predictor of the 0.23° × 0.31° model's response when considering the total number of directly identified tropical storm systems. However, comparison of the top row to the bottom row reveals that the 0.9° × 1.3° model's change in total tropical storm number does predict the sign of the 0.23° × 0.31° model's change in intense tropical cyclone number. This may very well be a consequence of the fixed thresholds chosen used in the storm detection and tracking scheme. The inability of the 0.9° × 1.3° model to produce sufficiently intense tropical storms implies that thresholds chosen based on actual storm properties will miss the weakest simulated systems biasing the identified set of storms to only the strongest ones that the model can produce (Walsh et al. 2007; Horn et al. 2014). This biased sample is then drawn from the tail of the full distribution, explaining the signs of the changes summarized in Table 1. We tested this hypothesis by reducing the wind speed threshold for storm detection from 17 to 12 m s^{-1}, resulting in 25% more identified storms in the CLIMO experiment using the 0.9° × 1.3° model. We further removed the warm core requirement in the detection algorithm, resulting in another 25% increase in identified storms. However, we

TABLE 1. A summary of the signs of the differences in the global average annual number of tropical storms between the four U.S. CLIVAR HWG idealized experiments as simulated by CAM5.1.

	SSTplus2_2xCO2 minus CLIMO	2xCO2 minus CLIMO	SSTplus2_2xCO2 minus SSTplus2	SSTplus2 minus CLIMO	SSTplus2_2xCO2 minus 2xCO2
0.9° × 1.3°, all TCs	Positive	Negative	Negative	Positive	Positive
0.23° × 0.31°, all TCs	Negative	Negative	Negative	Not significant	Negative
0.23° × 0.31°, categories 4–5	Positive	Negative	Negative	Positive	Positive

find that the percent changes in the perturbed experiments using either of these alternative storm tracking results are not significantly different from those shown in Fig. 2 using the Knutson et al. (2007) thresholds. Weak tropical storms are notoriously difficult to identify both in simulations (Li et al. 2013) and in observations (Landsea et al. 2010). If the model is indeed producing a sizable number of yet weaker tropical storms, it is not possible to robustly separate these storms from the background weather noise by varying only the threshold in this tracking scheme. However, the identified storms in the 0.9° × 1.3° model with relaxed thresholds resemble actual tropical storms even less so than the ones shown in Fig. 1, which tend to be too weak in intensity and too large in spatial scale. It is entirely possible that these unrealistic simulated storms respond to the U.S. CLIVAR HWG forcing changes in a different manner than the more realistic simulated storms in the 0.23° × 0.31° model. We conclude that due to either of these deficiencies, as in our previous study (Wehner et al. 2014), the 0.9° × 1.3° version of CAM5.1 is an inferior tool for simulating tropical storm statistics. As a result, conclusions regarding forced changes in tropical storm numbers obtained by direct sampling of storms from low-resolution CMIP5 climate models must be considered with caution. This is explored in detail by Camargo (2013), who analyzed tropical cyclone activity in various CMIP5 models. We also note that indirect methods of constructing tropical storm statistics from low-resolution climate models using large-scale climatological properties, such as in Emanuel et al. (2013), are not subject to this particular sampling bias.

4. Changes in tropical storm properties

As the climate changes, other properties of tropical storms besides the distribution of annual numbers may change. We focus our analysis in this section on the 0.23° × 0.31° model configuration due to its improved realism compared to the 0.9° × 1.3° model configuration.

Simulated tropical cyclones in the two experiments with increased SST exhibit longer durations than in the two experiments with 1990 climatological surface boundary conditions at the 0.23° × 0.31° model resolution. This increase occurs when the storms are at intensities of category 1 and above. The data in Fig. 5 labeled "Cat 0" shows that the average duration in days of all identified storms in the increased SST experiments with maximum winds between 17 and 33 m s^{-1} decreases slightly. However, the average duration of simulated storms at tropical cyclone strength or greater is lengthened by an increase in SST. The data labeled "Cat 1–3" shows the average duration of storms while the winds are 33 m s^{-1} but less than 58 m s^{-1}. Similarly, the data labeled "Cat 4–5" shows that the average duration of intense tropical cyclones (winds greater than 58 m s^{-1}) also increases.

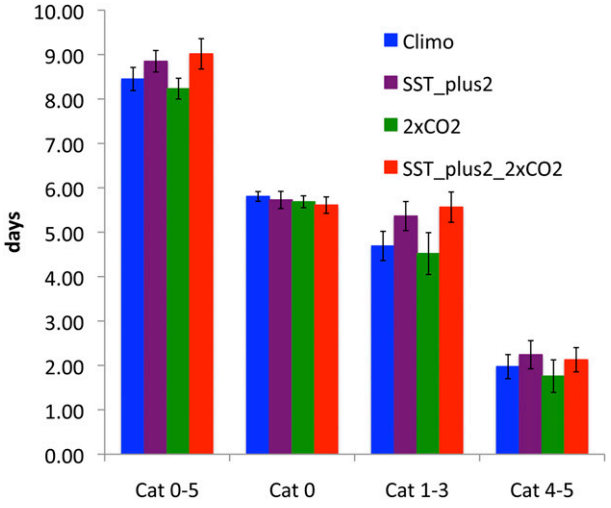

FIG. 5. Global average storm duration simulated by the 0.23° × 0.31° version of CAM5.1 for all tropical storms (categories 0–5), only tropical storms (category 0), tropical cyclones (categories 1 through 3), and intense tropical cyclones (categories 4 through 5). Error bars show the 5%–95% confidence interval based on the interannual variability of the average storm. Units: days.

From Fig. 5, the average duration per category 0 storm of winds decreases by ~5 h in the SSTplus2_2xCO2 experiment compared to the CLIMO experiment but this amount is only slightly larger than the ±4-h 95% confidence interval (based on the interannual variability of the average category 0 storm duration). The average duration of category 1–3 storms is simulated to be ~21 h longer and is significantly larger than the ±8-h 95% confidence interval. The average storm duration of winds at intense tropical cyclone strength or greater (≥ category 4) are simulated to last ~4 h longer, but the 95% confidence interval (±6.5 h) is larger than the difference. However, the effects of the two different forcing changes do not combine in a straightforward fashion. Storm duration changes are generally smaller in the SSTplus2 experiment (except for the most intense storms) but are of the same sign as in the SSTplus2_2xCO2 experiment. However, storm durations are decreased in all categories in the 2xCO2 experiment.

The total number of "storm days" per year is another measure of tropical storm activity and is a function of the number of storms and their average duration. Storm days, the sum of the duration of all storms of a given intensity over the year, is an alternative to the annual number of storms as a measure of the degree of tropical storm activity. The column labeled "Cat 0" in Fig. 6 shows the global average number of annual tropical

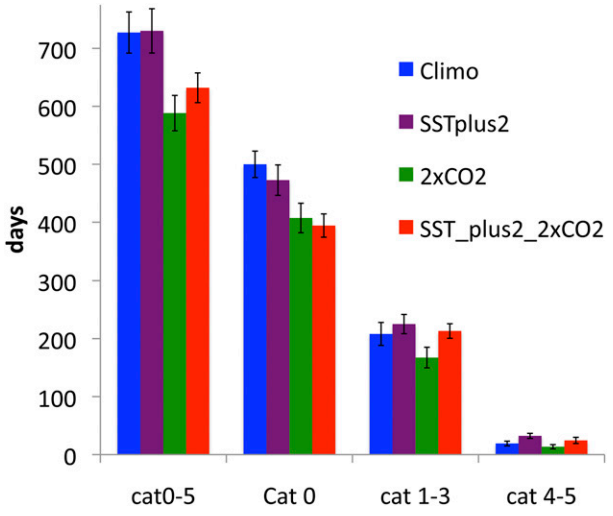

FIG. 6. Annual global average number of storm days simulated by the 0.23° × 0.31° version of CAM5.1, showing all storm days (categories 0–5), tropical storm days (category 0), tropical cyclone days (categories 1 through 3), and intense tropical cyclone days (categories 4 through 5). Error bars show the 5%–95% confidence interval based on the interannual variability. Units: days.

storm days. The annual number of tropical cyclone days is labeled "Cat 1–3" and the annual number of intense tropical cyclone days is labeled "Cat 4–5." This integrative measure of change in tropical storm activity reveals profound (~20%) and statistically significant decreases in tropical storm days in the SSTplus2 and SSTplus2_2xCO2 experiments due to the decrease in tropical storm number (Fig. 4) and their relatively unchanged duration (Fig. 5). The decrease in tropical cyclone number is more or less cancelled out by an increase in the duration of storms of this magnitude, resulting in a slight but not statistically significant increase in tropical cyclone days in the SSTplus2_2xCO2 experiment. However, the number of intense tropical cyclone days increases from 19 days in the CLIMO experiment to 25 days in the SSTplus2_2xCO2 experiment and this change is significant above the 90% level.

The averages of the maximum instantaneous precipitation rate as a function of storm intensity for the 0.23° × 0.31° model are shown in Fig. 7. This quantity was calculated by saving the maximum instantaneous precipitation rate for each identified storm followed by averaging across all storms within each Saffir–Simpson category. Both of the experiments with increased SST forcing exhibit statistically significant increases in maximum precipitation rates for all categories and range from 7% to 12% °C^{-1} of SST forcing. The Clausius–Clapeyron relation dictates that atmospheric moisture content changes by 6%–7% °C^{-1}. The exceedance of this constraint in simulated maximum precipitation rates suggests that a dynamical mechanism is also affected by the SST forcing. The doubling of CO_2 in these simulations produced no statistically significant changes in maximum instantaneous precipitation rate.

Shifts in the density of tropical cyclogenesis and storm tracks are exhibited to some degree in all three perturbed experiments. We calculated normalized genesis and track density for the 0.23° × 0.31° model by the method of Done et al. (2015) by counting the number of genesis points or tracks within 5° of each point on a 1° grid. Figure 8a shows the zonal average of the cyclogenesis density distribution for each of the four U.S. CLIVAR HWG experiments. In the Northern Hemisphere, the peak of this distribution shifts poleward from 10.5° to 12°N for the two warm experiments. No significant northern shift in seen in the 2xCO2 experiment. In the broader Southern Hemisphere part of the distribution, the peak shifts from 13°S to approximately 14°S for all three of the perturbed experiments. Poleward shifts are more evident in the zonal average distribution of cyclogenesis storm tracks density shown in Fig. 8b. In the Northern Hemisphere, a poleward shift in the peak of the track distribution from 14° to 16°N is exhibited by all three perturbed experiments. In the Southern Hemisphere, a similar shift from 13° to 17°S is exhibited by all three perturbed experiments. Maps of the cyclogenesis and track density are shown in the appendix (Figs. A4 and A5) as well as the changes in these densities for the perturbed experiments.

5. Changes in climatological tropical storm indices compared to tropical storm tracking results

The multivariate controls on tropical storm frequency and intensity have been distilled into single indices to better understand storm statistics. Emanuel (1986, 1987, 1995) developed the concept of maximum potential intensity (MPI), manifested by the maximum wind speed V_{max} and minimum central pressure P_{min} that could be achieved by a tropical storm if all the relevant large-scale conditions were ideal for cyclogenesis. These quantities, based on a model of the perfect storm as a Carnot engine, was further refined and detailed in Bister and Emanuel (1998, 2002a,b). Emanuel and Nolan (2004) further introduced a genesis potential index (GPI) based on this MPI defined as

$$\mathrm{GPI} = \frac{|10^5\eta|^{3/2}(H/50)^3(V_{max}/70)^3}{(1+0.1V_{shear})^2},$$

where is η the absolute vorticity at 850 hPa (in s^{-1}), H is the relative humidity at 600 hPa in percent, V_{max} is the

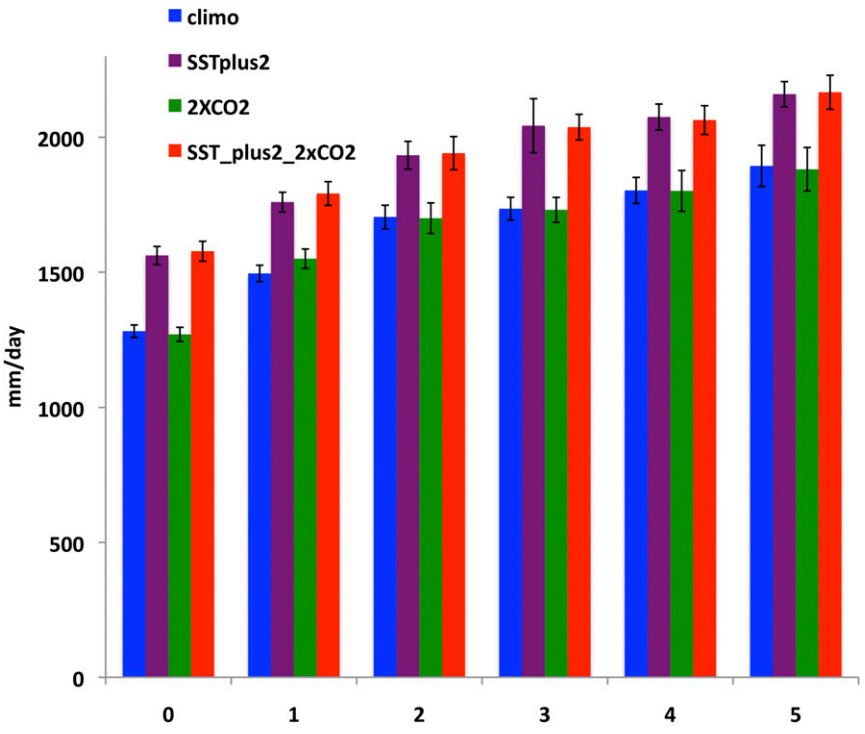

FIG. 7. Global average maximum instantaneous tropical storm precipitation as a function of intensity on the Saffir–Simpson scale simulated by the 0.23° × 0.31° version of CAM5.1 in the U.S. CLIVAR HWG configurations. Error bars show the 5%–95% confidence interval. Units: mm day^{-1}.

maximum potential intensity in m s^{-1}), and V_{shear} is the magnitude of the vertical wind shear between 850 and 200 hPa (in m s^{-1}).

Elaborated on in Camargo et al. (2007), the GPI is interpreted as a measure of the rate of cyclogenesis per unit area per unit time. Camargo et al. (2007) demonstrated that with the arbitrary but optimized set of constants in the formula for GPI, it adequately replicated the observed monthly climatology of tropical storm count when integrated over either hemispheres or ocean basins using the NCEP reanalysis. Following their example, we assess the changes in V_{max}, P_{min}, and GPI as simulated by CAM5.1 in the four U.S. CLIVAR experiments by driving Emanuel's code

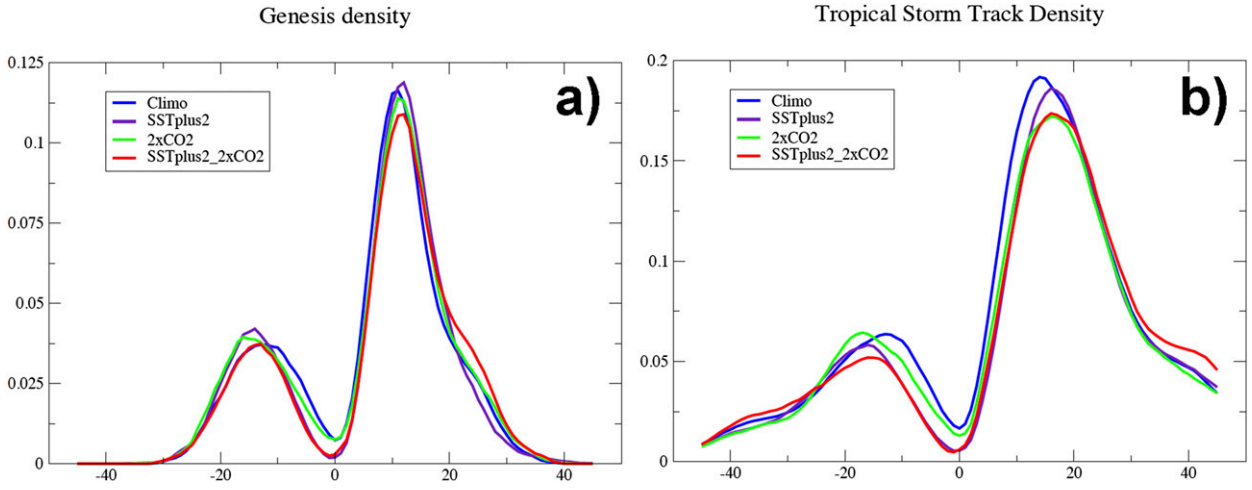

FIG. 8. Zonal average tropical storm (a) cyclogenesis and (b) track densities simulated by the 0.23° × 0.31° version of CAM5.1 in the U.S. CLIVAR HWG configurations.

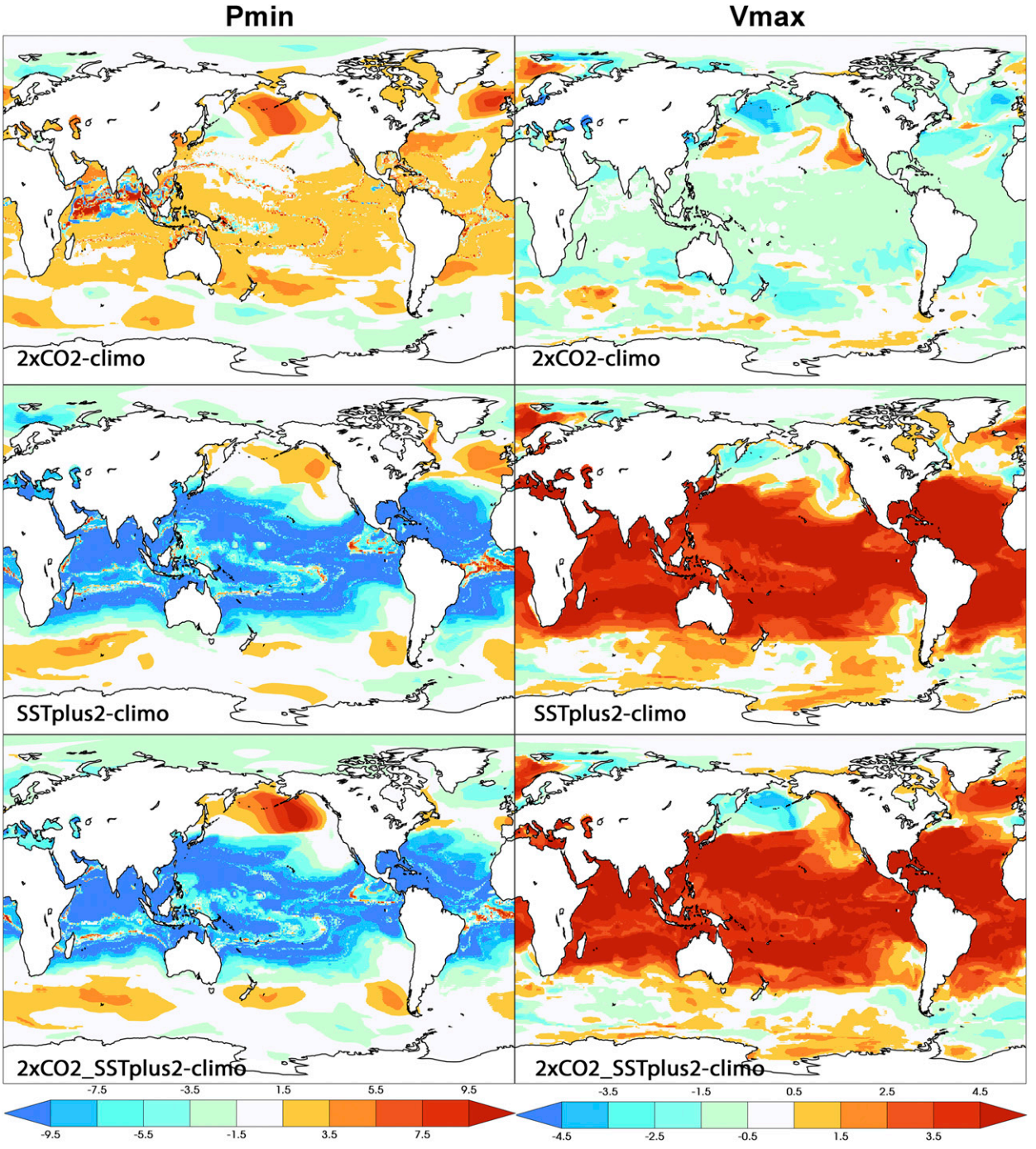

FIG. 9. Difference in annualized maximum potential intensity metrics of the perturbed U.S. CLIVAR HWG experiments from the CLIMO experiment produced by the 0.23° × 0.31° CAM5.1 configuration. Shown are (left) minimum central pressure (hPa) and (right) maximum wind speed (m s^{-1}), for (top) 2xCO2 minus CLIMO, (middle) SSTplus2 minus CLIMO, and (bottom) SSTplus2_2xCO2 minus CLIMO.

available online (ftp://texmex.mit.edu/pub/emanuel/TCMAX/pcmin_revised.f) with monthly mean input values to determine the MPI, followed by the definition of GPI given by Camargo et al. (2007).

Figure 9 shows the difference from the CLIMO experiment in V_{max} (right panels) and P_{min} (left panels) for the three perturbed experiments in the 0.23° × 0.31° CAM5.1 configuration. To annualize the monthly

TABLE 2. Simulated CAM5.1 changes in global average annual tracked global storm count, genesis potential index averaged over the global ocean, maximum potential wind, and minimum potential central pressures averaged from 40°S to 40°N and the top 10 lowest tracked pressures and highest tracked winds. Percent changes in pressure are relative to the annual mean sea level pressure P_{SL} for each experiment accounting for the slight increase in P_{SL} in a warmer climate. Pressure units are hectopascals. Wind speed units are meters per second.

	0.23° × 0.31°			0.9° × 1.3°		
	2xCO_2	SSTplus2	SSTplus2_2xCO_2	2xCO_2	SSTplus2	SSTplus2_2xCO_2
Δ No. of tracked storms	−14.5 (−17%)	−3.7 (−4%)	−15.8 (−18%)	−1.0 (−12%)	+2.8 (+33%)	+1.6 (+18%)
Δ GPI	−5.0 (−15%)	+9.6 (+30%)	+3.5 (+11%)	−5.5 (−14%)	+18.3 (+47%)	+11.5 (+29%)
Δ MPI P_{min}	+3.1 (+2.5%)	−17.6 (−11%)	−16.3 (−8.9%)	+1.7 (+2.5%)	−9.7 (−11%)	−9.0 (−9.4%)
Δ 10 lowest tracked pressures	+7.4 (+6%)	−11.3 (−7%)	−2.6 (−1.4%)			
Centered pattern correlation of Δ MPI P_{min} with 0.9° × 1.3°	0.20	0.79	0.77			
Δ MPI V_{max}	−1.7 (−1.3%)	+9.1 (+6.1%)	+8.2 (+5.2%)	−0.95 (−1.5%)	+4.8 (+6.7%)	+4.5 (+6.0%)
Δ 10 highest tracked winds	−1.4 (−2%)	+7.7 (+10%)	+5.0 (+7%)			
Centered pattern correlation of Δ MPI V_{max} with 0.9° × 1.3°	0.27	0.72	0.64			

measures of MPI, we calculated the maximum of V_{max} over the 12 months of each year, followed by the average over all simulated years. Similarly, we calculated the minimum of P_{min} over the 12 months of each year, followed by its average over all simulated years. Doubling of CO_2 alone (top panels) lowered V_{max} and raised P_{min} in the 0.23° × 0.31° version of CAM5.1, consistent in sign with the reduction in intense tropical cyclone frequency obtained from direct tracking of storms. Elevating the SST alone (middle panels) resulted in raising V_{max} and lowering P_{min}, also consistent with the increase in intense tropical cyclone frequency obtained from direct tracking of storms. Application of both forcing changes (lower panels) also resulted in raising V_{max} and lowering P_{min}, indicating that relative magnitudes of forced changes in MPI are consistent with interpretation of the direct tracking results. Table 2 compares changes in these bulk measures of maximum tropical storm potential intensities averaged from 40°S to 40°N with the change in the average of the 10 most intense simulated storms. While the relative magnitudes of the responses to the forcing changes are consistent for V_{max}, the bulk measures underestimate the response to CO_2 forcing relative to SST forcing for P_{min}. Table 2 also shows the percent change in V_{max} and P_{min}, the latter of which is calculated relative to the annual mean sea level pressure, P_{SL}, for each experiment accounting for the slight increase in P_{SL} in a warmer climate. Similar changes in these bulk potential intensity measures are found for the 0.9° × 1.3° CAM5.1 configuration and are shown in the appendix (Fig. A2). The magnitude of the 0.9° × 1.3° forced response in MPI is lower in all three experiments than in the 0.23° × 0.31° model as summarized in Table 2. Also, the 40°S–40°N pattern of the SST response is more similar between the two resolutions of CAM5.1 than the CO_2 response as measured by the centered pattern correlation (Houghton et al. 2001) shown in Table 2.

Figure 10 shows the difference from the CLIMO experiment in GPI for the perturbed experiments in the 0.23° × 0.31° CAM5.1 configuration. To annualize the monthly values of GPI, we summed the 12 monthly values for each year, followed by the average over all simulated years. In the Camargo et al. (2007) context, this value is interpreted as the density of the annual number of storms. Forced changes in GPI exhibit spatially mixed increases and decreases for each experiment. Doubling of CO_2 alone (upper left panel) decreased the global ocean basin average of GPI, consistent in sign but significantly lower in magnitude than the change in storm count from the tracking algorithm. However, elevating the SST alone (upper right panel) increased the global ocean basin average of GPI, a change opposite in sign to that obtained from the tracking algorithm. Hence, the experiment with both forcing changes (lower left panel) produced an increase in the global ocean basin average of GPI but a decrease in the total number of tracked storms in the 0.23° × 0.31° model configuration. It is important to note that while the global ocean basin average of GPI has increased for the experiment with both forcing changes, there is noticeable spatial variability in GPI and many areas do see decreases in GPI, mainly the Gulf of Mexico, Indian Ocean, and regions near the equator in the Pacific Ocean. Nonetheless, there is no significant correlation between GPI change in Fig. 10 and the change in density of

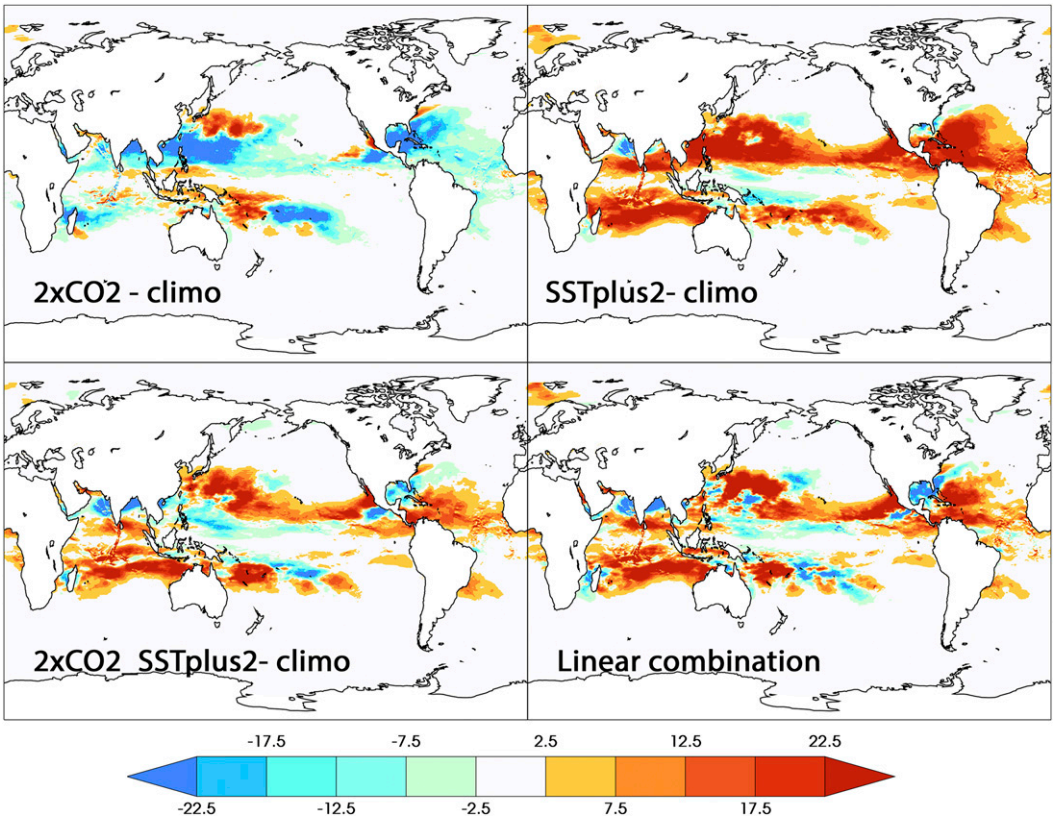

FIG. 10. Difference in annualized genesis potential index of the perturbed U.S. CLIVAR HWG experiments from the CLIMO experiment produced by the 0.23° × 0.31° CAM5.1 configuration: (top left) 2xCO2 minus CLIMO, (top right) SSTplus2 minus CLIMO, (bottom left) SSTplus2_2xCO2 minus CLIMO, and (bottom right) the sum of the two upper panels.

cyclogenesis (shown in Fig. A4) for any of the perturbed experiments.

Forced changes in GPI obtained from the 0.9° × 1.3° CAM5.1 configuration are shown in the appendix (Fig. A3). GPI simulated by the 0.9° × 1.3° model responded to the doubling of CO_2 alone in a remarkably similar manner to the 0.23° × 0.31° model. However, the increase in GPI due to elevated SST is far stronger in the 0.9° × 1.3° model than in the 0.23° × 0.31° model. Interestingly for either model resolution, the linear combination of the GPI changes in the SSTplus2 and 2xCO2 experiments is similar to that obtained from the SSTplus2_2xCO2 experiment and is indistinguishable in the average over global ocean basins. Likewise, such a linear combination of the global average tracked storm count changes also holds, despite the inconsistencies with GPI. The top two rows of Table 2 show the changes in annual tracked storm counts and the global ocean basin average of GPI for both model resolutions. An analysis of each of the four terms explicitly included in the GPI definition above reveals that, for the two warmer experiments, the contribution to GPI changes from the vorticity term are small and that the contribution from the wind shear term leads to a slight decrease. However, the contribution from both the relative humidity and the maximum potential intensity terms leads to increased GPI with the latter of these two dominating. The constants in the GPI formula, demonstrated by Camargo et al. (2007) to reproduce current observed cyclogenesis, contain implicit information about the number of localized vorticity disturbances necessary to initiate cyclogenesis and the efficiency into which they evolve into tropical storms. The discrepancy between the changes in the number of explicitly tracked storms in 0.23° × 0.31° model and its GPI change indicates that these constants are not appropriate for the two warmer experiments, leading to the possibility that the number of localized disturbances or the rate at which they evolve into tropical storms changes in a warmer climate. We note that the vorticity term used in the GPI definition is calculated from monthly mean zonal and meridional wind components and is quite different than the monthly mean of the instantaneous vorticity itself and may not adequately represent the effect of the short-duration disturbances.

Along these lines, Zhao and Held (2012) suggested vertical convective mass flux as a predictor for changes in cyclogenesis. While not a perfect proxy for vertical convective mass flux, they found that changes in ω_{500}, the 500-hPa vertical pressure velocity, were highly correlated to changes in cyclogenesis in their model in all ocean basins. For the 0.23° × 0.31° version of CAM5.1, the global annual average ω_{500} decreases by approximately ⅓ in the both the SSTplus2 and 2xCO2 experiments relative to the CLIMO experiment when weighted by each experiment's cyclogenesis density described above. The SSTplus2_2xCO2 experiment exhibits a 50% decrease when averaged in this manner. Comparison of the relative magnitude of these weighted ω_{500} changes with the actual changes in the number of tropical storms in Fig. 4 and Table 2 suggests that this metric reproduces the sign but not the relative magnitude of the reduction for the three U.S. CLIVAR HWG forcings. Furthermore, we find a modest correlation (0.5) between reduced ω_{500} and cyclogenesis density only in the eastern Pacific basin in the two warmed experiments of the 0.23° × 0.31° model presented here. In other regions of reduced cyclogenesis, ω_{500} either increases slightly or does not change appreciably, resulting in no significant correlation (not shown). One interpretation of this analysis is that while the large-scale meteorological patterns may be more favorable for tropical cyclogenesis in the warmer experiments, fewer tropical storms actually form due to the lack of initiation events and the fact that more skillful projections of future cyclogenesis from these patterns alone will require higher-frequency information than monthly means. However, placement of high confidence in this interpretation would require the discovery of a relationship between changes in high-frequency variability and changes in cyclogenesis that remains elusive at this point.

6. Conclusions

Integration of the four idealized experiments defined by the U.S. CLIVAR Hurricane Working Group by the Community Atmospheric Model (CAM5.1) at two different horizontal resolutions produce very different forced responses in their tropical storm statistics. Using the same tropical storm tracking algorithm and threshold parameters, far fewer storms are identified in the baseline 0.9° × 1.3° model configuration than in the 0.23° × 0.31° configuration. Both model configurations produce fewer total annual numbers of tropical storms when CO_2 is increased without any changes in surface ocean temperatures. However, the model's response to a uniform 2°C increase in SST varies in sign for the total annual number of tropical storms between the two configurations with the 0.9° × 1.3° model exhibiting an increase and the 0.23° × 0.31° model exhibiting a decrease. This discrepancy between model configurations persists when both forcing changes are applied and may be a consequence of the methods used in this study to count and track tropical storms. Because the thresholds in the tracking algorithm are appropriate for models that simulate tropical storms of realistic intensities, many, if not most, cyclonic features in the tropics produced by the 0.9° × 1.3° model are not identified. Thus, the storms that are identified in the coarser model simulation represent the model's most intense storms. In this interpretation, the 0.9° × 1.3° model's total storm count change is a good predictor for the 0.23° × 0.31° model's intense storm count change but not its total storm count change. On the other hand, the storms that are identified in the 0.9° × 1.3° model, particularly when the tracking algorithm thresholds are relaxed, are not physically realistic tropical storms. Hence, confidence that the forced response of such events bears a resemblance to reality is undermined. As noted above, the tropical storm frequency and intensity of the few models that have been studied at high resolution for tropical storm behavior exhibit substantially different convergence properties. It is quite likely that the forced response in tropical storm frequency and intensity also differs substantially across high-resolution climate models. Nonetheless, the difficulties encountered in this study with CAM5.1 illustrate that interpretations of the effect of climate change on tropical storm statistics from CMIP3/5 class resolution models may not extend to higher-resolution versions of the same models.

The greater realism of both tropical storm intensities and their statistics in the 0.23° × 0.31° configuration of CAM5.1 allows a number of interesting conclusions to be drawn about the behavior of the *model* under oversimplified forcing changes. We note that great caution should be taken in the connection of model behavior to real-world behavior, as a number of important model biases are present. Principal among these is that convergence of tropical storm properties with resolution has not yet been demonstrated. The response of 0.23° × 0.31° model to the U.S. CLIVAR HWG forcings reconfirms previous results from two other high-resolution global atmospheric models (Held and Zhao 2011; Sugi et al. 2012) in that both a uniform increased SST and elevated CO_2 change separately lead to a global reduction in tropical storm frequency. However, in the results presented here, the CO_2 effect is substantially larger than the SST effect whereas in the other models the effects were roughly equal.

A simple spatially uniform increase in SST is not a realistic projection of the future anthropogenic climate change. The spatial structure of projected future SSTs

varies significantly across the CMIP5 models, even for a similar amount of global warming. The tropical cyclone response of the 0.23° × 0.31° configuration CAM5.1 to such heterogeneous surface forcing changes is likely to be dependent on the model's bias in cyclogenesis location.

The 0.23° × 0.31° model's change (~40%) in the total annual number of simulated intense tropical storms by only increasing the SST by 2°C would appear to be similar to the 25%–30% °C^{-1} found in observations by Holland and Bruyère (2014). However, increasing both atmospheric CO_2 and SST yields a net model sensitivity of approximately +10% °C^{-1} for intense tropical storm count. This larger difference from observations could be a result of the model bias in simulating the number of intense tropical storms (~10 per year for the model versus ~15 per year for the real world). Another possible cause could be that the combination of forcings in the numerical experiment is not consistent with the real-world climate sensitivity.

In the 0.23° × 0.31° model, the average duration of simulated weak storms (category 0) is not sensitive to the forcing changes in the U.S. CLIVAR HWG experiments. The average duration of simulated tropical cyclones (categories 1–5) is lengthened by increases in SST. Translational speeds of category 1–3 storms are found to be insensitive to these forced changes (not shown). However, simulated intense tropical cyclones travel slightly faster in the warmer experiments. Hence, the total distance traveled by tropical cyclones is greater in warmer simulations. Extension of tropical cyclones tracks to both lower and high latitudes occurs but varies substantially between ocean basins. The simulated change in the total number of annual "storm days" is a strong function of storm intensity with significant decreases for tropical storms and significant increases for intense tropical cyclones. The latter change could have important societal ramifications, as the risk of experiencing intense tropical cyclones would be increased if this change occurred for landfalling storms in the real world.

The physical mechanisms causing these complicated changes in simulated tropical storm behavior in the U.S. CLIVAR HWG experiments are difficult to connect to the forced changes in the model's climatology. Increases in available energy and moisture in the increased SST are likely responsible for a simulated shift toward more intense storms in the 0.23° × 0.31° version of CAM5.1. Changes in Emanuel's MPI are entirely consistent with that produced by the model in terms of both V_{max} and P_{min} for the two warmer configurations. Emanuel and Nolan's genesis potential index successfully reflects the 0.23° × 0.31° model's decrease in total global annual tropical storm number in the 2xCO2 experiment but predicts an increase rather than the decrease that is actually simulated in either experiment where 2°C is uniformly added to the sea surface temperature.

The maximum local instantaneous precipitation associated with tropical storms in the 0.23° × 0.31° model increases with SST slightly in exceedance with that expected from the Clausius–Clapeyron relationship for all simulated storm intensities. Villarini et al. (2014) found that total simulated tropical storm precipitation in this and other models increased consistently with the Clausius–Clapeyron relationship. However, Knutson et al. (2013) showed that precipitation increases within 200 km of tropical storm centers exceeded this constraint in downscaled projections of CMIP3/5 simulations. Hence it is possible that changes in convergent dynamical mechanisms in the most intense regions of tropical storms are also affecting changes in local moisture content and precipitation.

While the simplified forcing changes specified in U.S. CLIVAR Hurricane Working Group's protocols do reveal some interesting behaviors in the response of tropical storms, they do not fully inform how future tropical storms might change in high-resolution fully coupled models or in the real world as the composition of the atmosphere changes. There is ample evidence that the pattern of sea surface temperature change is an important controlling factor in tropical storm frequency (Zhao et al. 2012). Future coordinated experimentation should explore the variety of projected SST patterns in the CMIP5 archive. Furthermore, the infinite ocean heat capacity represented in stand-alone atmospheric model experiments precludes important air–sea interactions that affect tropical storm intensity (Schade and Emanuel 1999; Knutson et al. 2001; Lin et al. 2013). While high-resolution fully coupled models are currently too computationally expensive to spin up the ocean state, slab or mixed layer ocean models can provide some of these interactions and could serve as an intermediate step until high-performance computing technology permits routine integration of tropical cyclone permitting fully coupled climate models.

Acknowledgments. This work was supported by the Regional and Global Climate Modeling Program of the Office of Biological and Environmental Research in the U.S. Department of Energy Office of Science under Contract DE-AC02-05CH11231. Calculations were performed at the National Energy Research Supercomputing Center (NERSC) at the Lawrence Berkeley National Laboratory. We thank the anonymous reviewers for their thorough review comments which we feel substantially improved the study.

APPENDIX

Additional Figures and Table

Figure A1 shows an observational estimate of tropical storm tracks. Comparison to the high-resolution model results of Fig. 3a reveals the largest bias to be in the central Pacific basin.

Figures A2 and A3 show the changes in MPI and GPI for the low-resolution model. Comparison to the high-resolution model changes in Figs. 9 and 10 reveals that these measures of model projections are robust to resolution.

Figures A4 and A5 show changes in tropical storm cyclogenesis and track densities for the high-resolution model. Details of these changes by tropical storm intensity are summarized in Table A1.

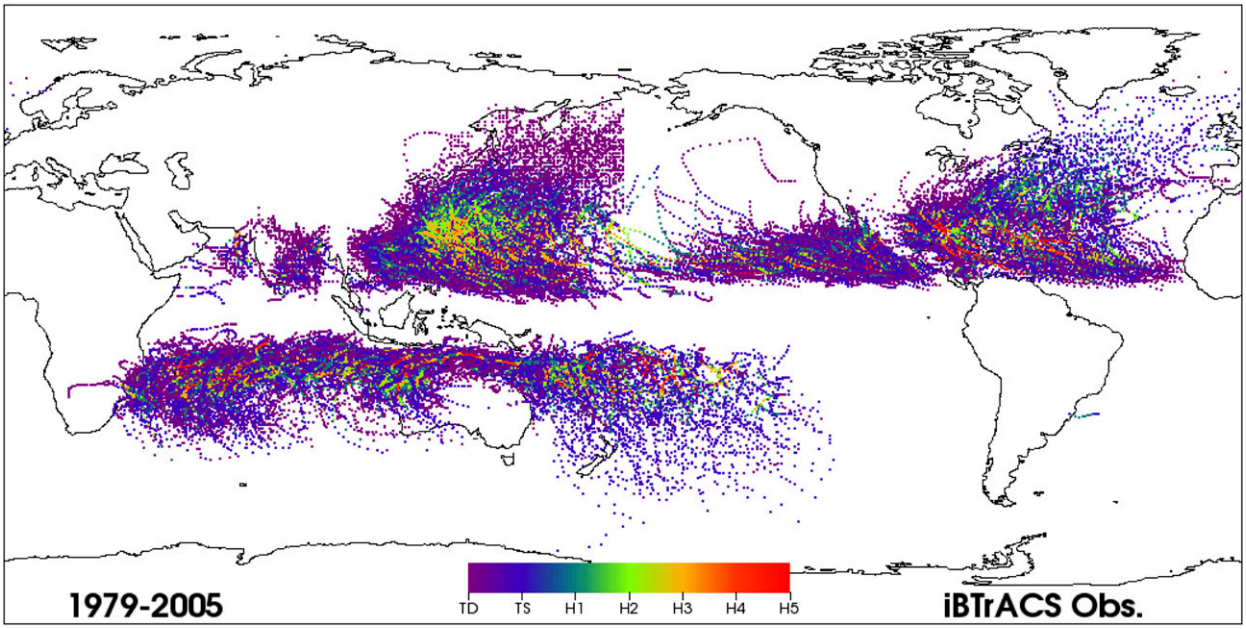

FIG. A1. Observed tropical storm tracks from Emanuel over the period 1979–2005. Colors indicate maximum wind speeds on the Saffir–Simpson scale.

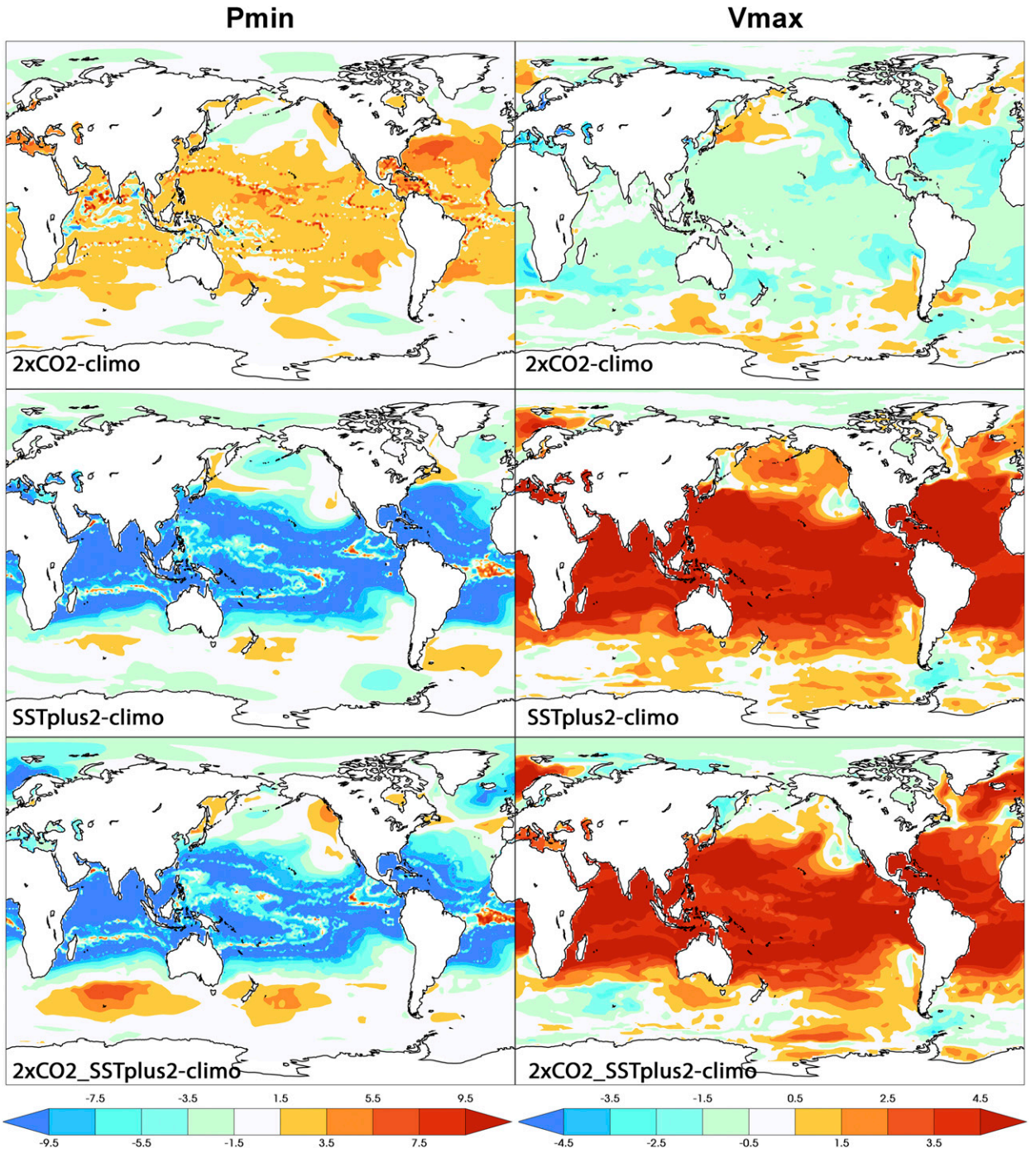

FIG. A2. Difference in annualized maximum potential intensity metrics of the perturbed U.S. CLIVAR HWG experiments from the CLIMO experiment produced by the 0.9° × 1.3° CAM5.1 configuration: (left) minimum central pressure (hPa) and (right) maximum wind speed ($m\,s^{-1}$), for (top) 2xCO2 minus CLIMO, (middle) SSTplus2 minus CLIMO, and (bottom) SSTplus2_2xCO2 minus CLIMO.

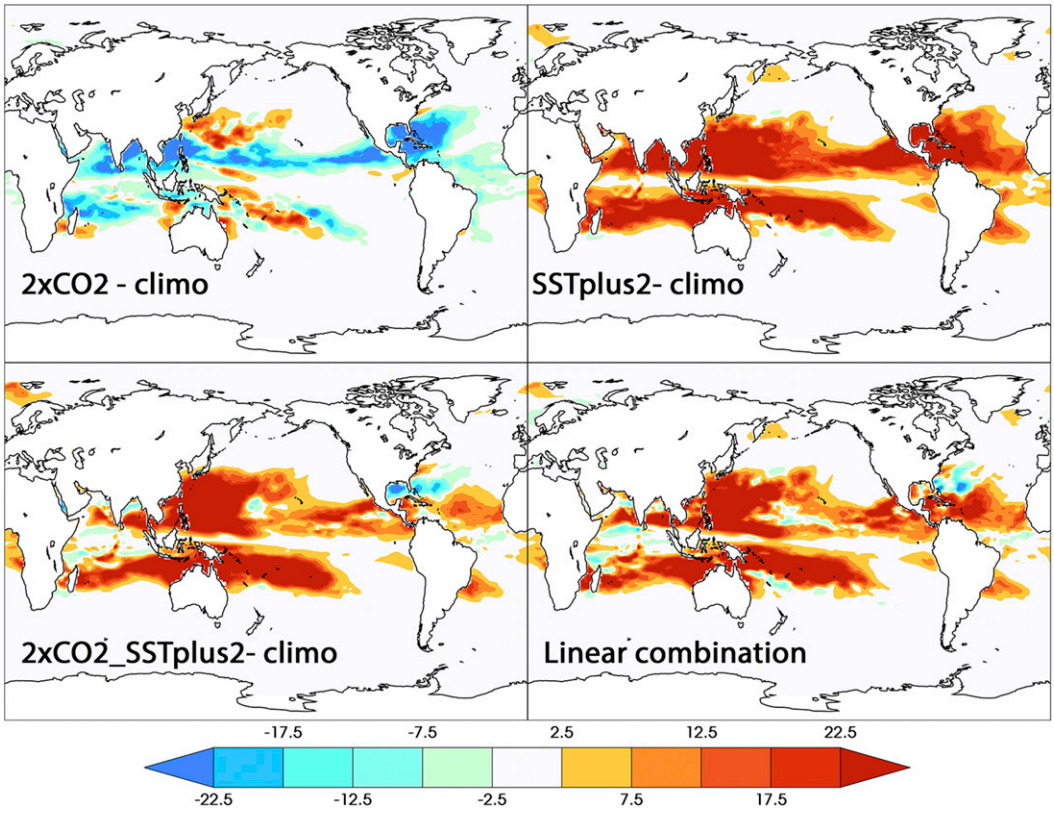

FIG. A3. Difference in annualized genesis potential index of the perturbed U.S. CLIVAR HWG experiments from the CLIMO experiment produced by the 0.9° × 1.3° CAM5.1 configuration: (top left) 2xCO2 minus CLIMO, (top right) SSTplus2 minus CLIMO, (bottom left) SSTplus2_2xCO2 minus CLIMO, and (bottom right) the sum of the two upper panels.

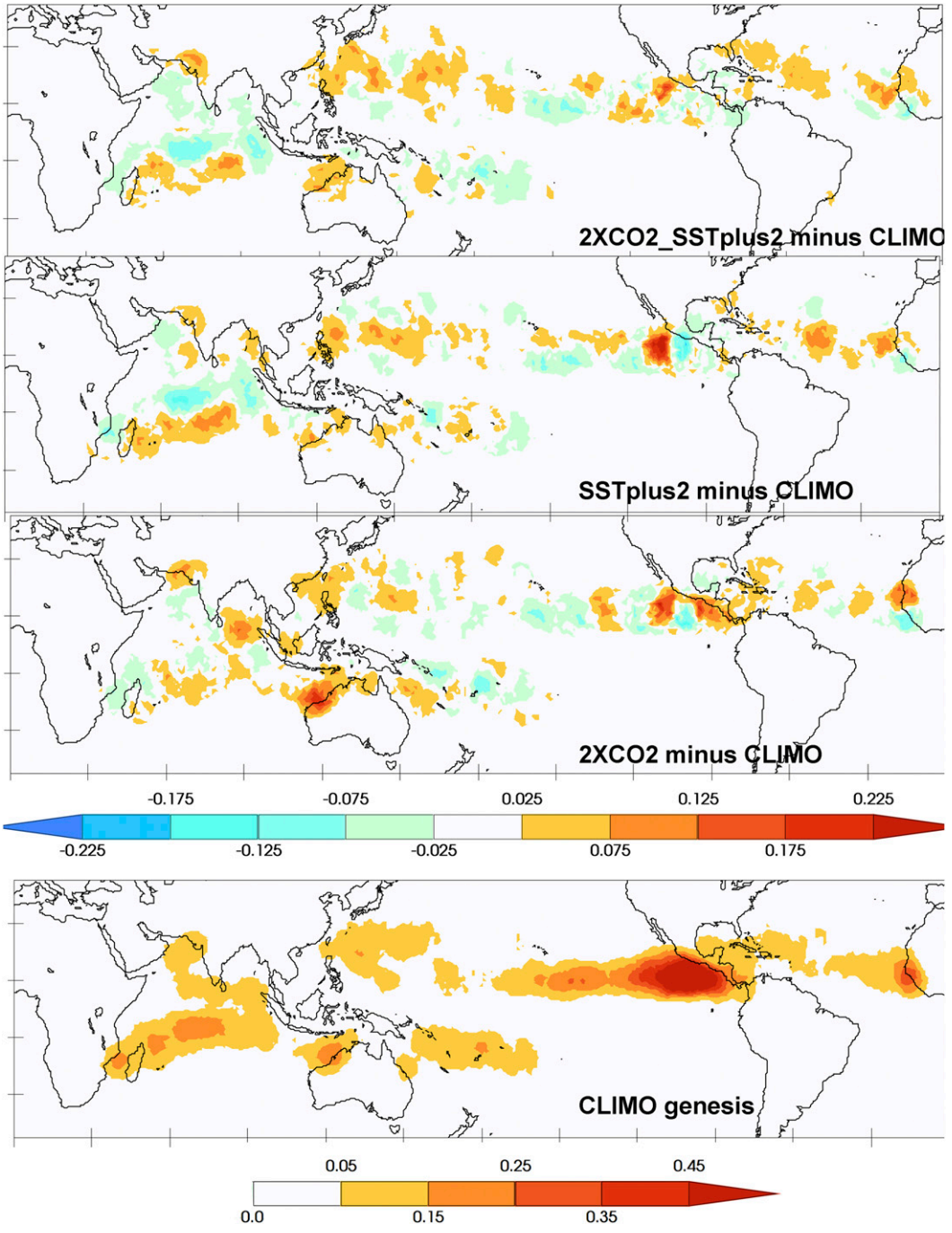

FIG. A4. (bottom) Tropical storm cyclogenesis density simulated by the 0.23° × 0.31° version of CAM5.1 in the U.S. CLIVAR HWG CLIMO experiment, and (top) the differences from the CLIMO experiment for the three perturbed U.S. CLIVAR HWG experiments.

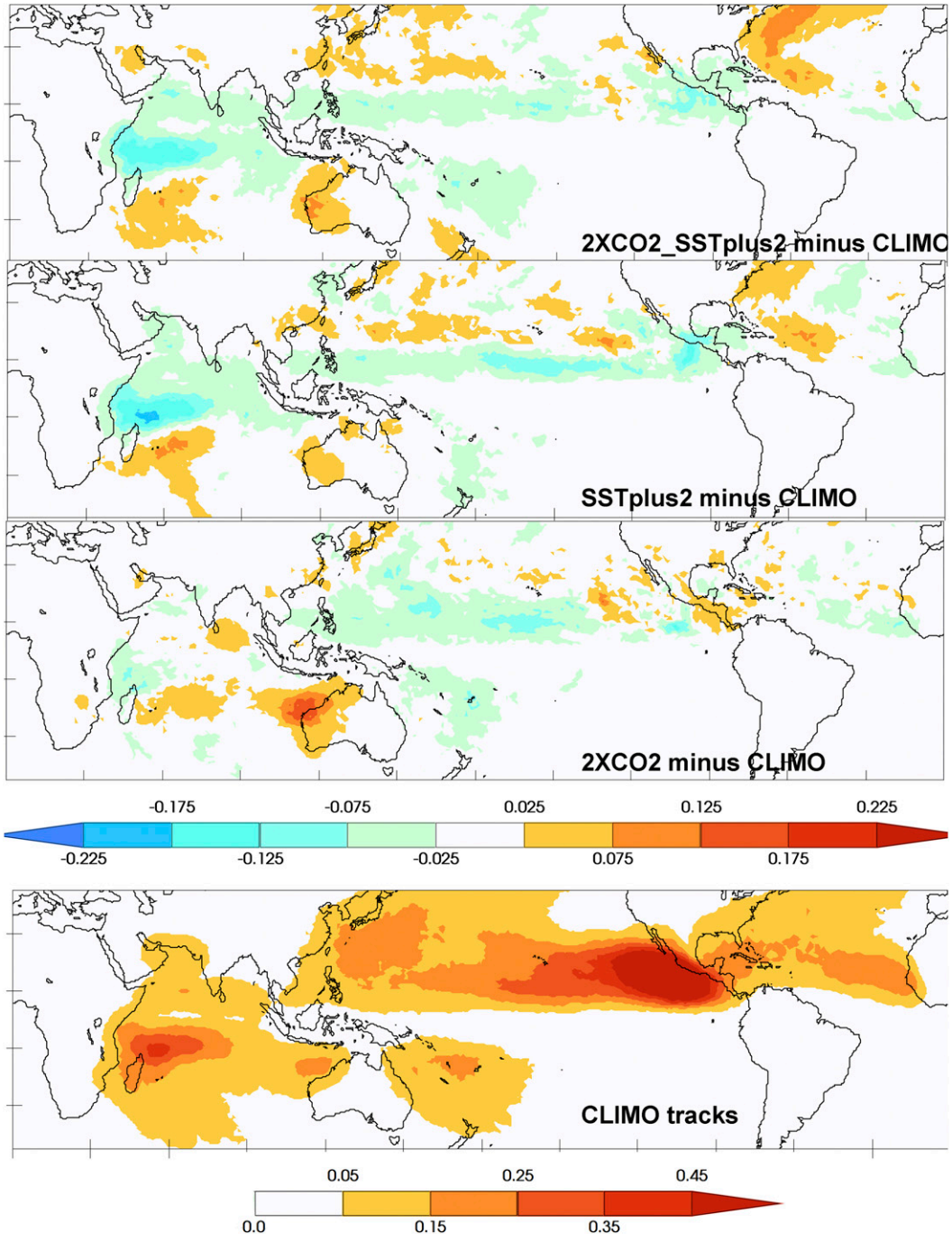

FIG. A5. As in Fig. A4, but for tropical storm track density.

TABLE A1. A summary of the changes in global tropical storm statistics for the 0.23° × 0.31° CAM5.1 configuration. Results are shown as the difference of the perturbed experiments from the CLIMO experiment. Differences significant above the 90% level using a two-sided *t* test are indicated in boldface font.

	$2xCO_2$				SSTplus2				SSTplus2_$2xCO_2$			
Category	0–5	0	1–3	4–5	0–5	0	1–3	4–5	0–5	0	1–3	4–5
Δ annual storm count	**−15**	**−5**	**−7**	**−2**	−4	**−6**	−2	**5**	**−16**	**−12**	**−6**	2
Δ average storm length	−5	−3	−4	−5	**10**	−2	**16**	**6**	**19**	**−5**	**21**	4
Δ annual storm days	**−139**	**−93**	**−41**	**−6**	3	−27	17	**13**	**−95**	**−106**	5	5

REFERENCES

Bacmeister, J. T., M. F. Wehner, R. B. Neale, A. Gettelman, C. Hannay, P. H. Lauritzen, J. M. Caron, and J. E. Truesdale, 2014: Exploratory high-resolution climate simulations using the Community Atmosphere Model (CAM). *J. Climate,* **27,** 3073–3099, doi:10.1175/JCLI-D-13-00387.1.

Bister, M., and K. A. Emanuel, 1998: Dissipative heating and hurricane intensity. *Meteor. Atmos. Phys.,* **65,** 233–240, doi:10.1007/BF01030791.

——, and ——, 2002a: Low frequency variability of tropical cyclone potential intensity. 1. Interannual to interdecadal variability. *J. Geophys. Res.,* **107,** 4801, doi:10.1029/2001JD000776.

——, and ——, 2002b: Low frequency variability of tropical cyclone potential intensity. 2. Climatology for 1982–1995. *J. Geophys. Res.,* **107,** 4621, doi:10.1029/2001JD000780.

Camargo, S. J., 2013: Global and regional aspects of tropical cyclone activity in the CMIP5 models. *J. Climate,* **26,** 9880–9902, doi:10.1175/JCLI-D-12-00549.1.

——, K. A. Emanuel, and A. B. Sobel, 2007: Use of a genesis potential index to diagnose ENSO effects on tropical cyclone genesis. *J. Climate,* **20,** 4819–4834, doi:10.1175/JCLI4282.1.

Christensen, J. H., and Coauthors, 2013: Climate phenomena and their relevance for future regional climate change. *Climate Change 2013: The Physical Science Basis,* T. F. Stocker et al., Eds., Cambridge University Press, 1217–1308.

Daloz, A. S., and Coauthors, 2015: Cluster analysis of downscaled and explicitly simulated North Atlantic tropical cyclone tracks. *J. Climate,* **28,** 1333–1361, doi:10.1175/JCLI-D-13-00646.1.

Done, J., G. Holland, C. Bruyère, L. Leung, and A. Suzuki-Parker, 2015: Modeling high-impact weather and climate: Lessons from a tropical cyclone perspective. *Climatic Change,* doi:10.1007/s10584-013-0954-6, in press.

Emanuel, K. A., 1986: An air–sea interaction theory for tropical cyclones. Part I: Steady-state maintenance. *J. Atmos. Sci.,* **43,** 585–604, doi:10.1175/1520-0469(1986)043<0585:AASITF>2.0.CO;2.

——, 1987: The dependence of hurricane intensity on climate. *Nature,* **326,** 483–485, doi:10.1038/326483a0.

——, 1995: Sensitivity of tropical cyclones to surface exchange coefficients and a revised steady-state model incorporating eye dynamics. *J. Atmos. Sci.,* **52,** 3969–3976, doi:10.1175/1520-0469(1995)052<3969:SOTCTS>2.0.CO;2.

——, 2013: Downscaling CMIP5 climate models shows increased tropical cyclone activity over the 21st century. *Proc. Natl. Acad. Sci. USA,* **110,** 12 219–12 224, doi:10.1073/pnas.1301293110.

——, and D. S. Nolan, 2004: Tropical cyclone activity and global climate. Preprints, *26th Conf. on Hurricanes and Tropical Meteorology,* Miami, FL, Amer. Meteor. Soc., 240–241.

Held, I. M., and M. Zhao, 2011: The response of tropical cyclone statistics to an increase in CO_2 with fixed sea surface temperatures. *J. Climate,* **24,** 5353–5364, doi:10.1175/JCLI-D-11-00050.1.

Hodges, K. I., 1996: Spherical nonparametric estimators applied to the UGAMP model integration for AMIP. *Mon. Wea. Rev.,* **124,** 2914–2932, doi:10.1175/1520-0493(1996)124<2914:SNEATT>2.0.CO;2.

Holland, G., and C. L. Bruyère, 2014: Recent intense hurricane response to global climate change. *Climate Dyn.,* **42,** 617–627, doi:10.1007/s00382-013-1713-0.

Horn, M., and Coauthors, 2014: Tracking scheme dependence of simulated tropical cyclone response to idealized climate simulations. *J. Climate,* **27,** 9197–9213, doi:10.1175/JCLI-D-14-00200.1.

Houghton, J. T., Y. Ding, D. J. Griggs, M. Noguer, P. J. van der Linden, X. Dai, K. Maskell, and C. A. Johnson, Eds., 2001: *Climate Change 2001: The Scientific Basis.* Cambridge University Press, 881 pp. [See appendix 12.3 therein for a discussion of pattern correlation.]

Knapp, K. R., M. C. Kruk, D. H. Levinson, H. J. Diamond, and C. J. Neumann, 2010: The International Best Track Archive for Climate Stewardship (IBTrACS): Unifying tropical cyclone best track data. *Bull. Amer. Meteor. Soc.,* **91,** 363–376, doi:10.1175/2009BAMS2755.1.

Knutson, T. R., R. E. Tuleya, W. Shen, and I. Ginis, 2001: Impact of CO_2-induced warming on hurricane intensities as simulated in a hurricane model with ocean coupling. *J. Climate,* **14,** 2458–2468, doi:10.1175/1520-0442(2001)014<2458:IOCIWO>2.0.CO;2.

——, J. J. Sirutis, S. T. Garner, I. Held, and R. E. Tuleya, 2007: Simulation of the recent multidecadal increase of Atlantic hurricane activity using an 18-km-grid regional model. *Bull. Amer. Meteor. Soc.,* **88,** 1549–1565, doi:10.1175/BAMS-88-10-1549.

——, and Coauthors, 2010: Tropical cyclones and climate change. *Nat. Geosci.,* **3,** 157–163, doi:10.1038/ngeo779.

——, and Coauthors, 2013: Dynamical downscaling projections of twenty-first-century Atlantic hurricane activity: CMIP3 and CMIP5 model-based scenarios. *J. Climate,* **26,** 6591–6617, doi:10.1175/JCLI-D-12-00539.1.

Landsea, C. W., G. A. Vecchi, L. Bengtsson, and T. R. Knutson, 2010: Impact of duration thresholds on Atlantic tropical cyclone counts. *J. Climate,* **23,** 2508–2519, doi:10.1175/2009JCLI3034.1.

Li, F., W. D. Collins, M. F. Wehner, and R. L. Leung, 2013: Hurricanes in an aquaplanet world: Implications of the impacts of external forcing and model horizontal resolution. *J. Adv. Model. Earth Syst.,* **5,** 134–145, doi:10.1002/jame.20020.

Lin, I., and Coauthors, 2013: An ocean coupling potential intensity index for tropical cyclones. *Geophys. Res. Lett.,* **40,** 1878–1882, doi:10.1002/grl.50091.

Murakami, H., and Coauthors, 2012: Future changes in tropical cyclone activity projected by the new high-resolution MRI-AGCM. *J. Climate,* **25,** 3237–3260, doi:10.1175/JCLI-D-11-00415.1.

Neale, R. B., and Coauthors, 2010: Description of the NCAR Community Atmosphere Model (CAM 5.0). NCAR Tech. Note NCAR/TN-486+STR, 282 pp.

Oouchi, K., J. Yoshimura, H. Yoshimura, R. Mizuta, S. Kusonoki, and A. Noda, 2006: Tropical cyclone climatology in a global-warming climate as simulated in a 20-km mesh global atmospheric model: Frequency and wind intensity analyses. *J. Meteor. Soc. Japan,* **84,** 259–276, doi:10.2151/jmsj.84.259.

Prabhat, O. Rübel, S. Byna, K. Wu, F. Li, M. Wehner, and W. Bethel, 2012: TECA: A Parallel Toolkit for Extreme Climate Analysis. *Procedia Comput. Sci.,* 9. 866–876, doi:10.1016/j.procs.2012.04.093.

Reed, K. A., and C. Jablonowski, 2011a: An analytic vortex initialization technique for idealized tropical cyclone studies in AGCMs. *Mon. Wea. Rev.,* **139,** 689–710, doi:10.1175/2010MWR3488.1.

——, and ——, 2011b: Assessing the uncertainty of tropical cyclone simulations in NCAR's Community Atmosphere Model. *J. Adv. Model. Earth Syst.,* **3,** M08002, doi:10.1029/2011MS000076.

——, ——, and M. A. Taylor, 2012: Tropical cyclones in the spectral element configuration of the Community Atmosphere Model. *Atmos. Sci. Lett.,* **13,** 303–310, doi:10.1002/asl.399.

Schade, L. R., and K. E. Emanuel, 1999: The ocean's effect on the intensity of tropical cyclones: Results from a simple coupled atmosphere–ocean model. *J. Atmos. Sci.,* **56,** 642–651, doi:10.1175/1520-0469(1999)056<0642:TOSEOT>2.0.CO;2.

Shaevitz, D. A., and Coauthors, 2014: Characteristics of tropical cyclones in high-resolution models of the present climate. *J. Adv. Model. Earth Syst.,* **6,** 1154–1172, doi:10.1002/2014MS000372.

Strachan, J., P. L. Vidale, K. Hodges, M. Roberts, and M.-E. Demory, 2013: Investigating global tropical cyclone activity with a hierarchy of AGCMs: The role of model resolution. *J. Climate,* **26,** 133–152, doi:10.1175/JCLI-D-12-00012.1.

Sugi, M., H. Murakami, and J. Yoshimura, 2009: A reduction in global tropical cyclone frequency due to global warming. *SOLA,* **5,** 164–167.

——, ——, and ——, 2012: On the mechanism of tropical cyclone frequency changes due to global warming. *J. Meteor. Soc. Japan,* **90A,** 397–408, doi:10.2151/jmsj.2012-A24.

Villarini, G., D. A. Lavers, E. Scoccimarro, M. Zhao, M. F. Wehner, G. A. Vecchi, T. R. Knutson, and K. A. Reed, 2014: Sensitivity of tropical cyclone rainfall to idealized global-scale forcings. *J. Climate,* **27,** 4622–4641, doi:10.1175/JCLI-D-13-00780.1.

Walsh, K. J. E., M. Fiorino, C. W. Landsea, and K. L. McInnes, 2007: Objectively determined resolution-dependent threshold criteria for the detection of tropical cyclones in climate models and reanalyses. *J. Climate,* **20,** 2307–2314, doi:10.1175/JCLI4074.1.

——, and Coauthors, 2015: Hurricanes and climate: The U.S. CLIVAR working group on hurricanes. *Bull. Amer. Meteor. Soc.*, doi:10.1175/BAMS-D-13-00242.1, in press.

Wehner, M. F., and Coauthors, 2014: The effect of horizontal resolution on simulation quality in the Community Atmospheric Model, CAM5.1. *J. Adv. Model. Earth Syst.,* **6,** 980–997, doi:10.1002/2013MS000276.

Yamada, Y., K. Oouchi, M. Satoh, H. Tomita, and W. Yanase, 2010: Projection of changes in tropical cyclone activity and cloud height due to greenhouse warming: Global cloud-system-resolving approach. *Geophys. Res. Lett.,* **37,** L07709, doi:10.1029/2010GL042518.

Yoshimura, J., and M. Sugi, 2005: Tropical cyclone climatology in a high-resolution AGCM—Impacts of SST warming and CO_2 increase. *SOLA,* **1,** 133–136.

Zhao, M., and I. M. Held, 2012: TC-permitting GCM simulations of hurricane frequency response to sea surface temperature anomalies projected for the late-twenty-first century. *J. Climate,* **25,** 2995–3009, doi:10.1175/JCLI-D-11-00313.1.

——, ——, S.-J. Lin, and G. A. Vecchi, 2009: Simulations of global hurricane climatology, interannual variability, and response to global warming using a 50-km resolution GCM. *J. Climate,* **22,** 6653–6678, doi:10.1175/2009JCLI3049.1.

——, ——, and ——, 2012: Some counterintuitive dependencies of tropical cyclone frequency on parameters in a GCM. *J. Atmos. Sci.,* **69,** 2272–2283, doi:10.1175/JAS-D-11-0238.1.

——, and Coauthors, 2013: Robust direct effect of increasing atmospheric CO2 concentration on global tropical cyclone frequency—A multi-model inter-comparison. *U.S. CLIVAR Variations,* No. 11 (3), U.S. CLIVAR Project Office, Washington, DC, 17–23.